Proton-Proton and Proton-Neutron Correlations in Medium-Weight Nuclei: Role of the Tensor Force within a Many-Body Cluster Expansion

M. Alvioli* - C. Ciofi degli Atti* - H. Morita**

* Department of Physics, University of Perugia and INFN, Sezione di Perugia
** Sapporo Gakuin University, Hokkaido, Japan

Abstract. – *A detailed analysis of the effect of tensor correlations on one- and two-body densities and momentum distributions of complex nuclei is presented within a linked cluster expansion providing reliable results for the ground state properties of nuclei calculated with realistic interactions.*

Obtaining information on short range nucleon-nucleon correlations (SRC) in nuclei is a primary goal of modern nuclear physics. The interest in SRC stems not only from the necessity to firmly establish the limits of validity of the standard model of nuclei but also from the strong impact that the knowledge of the short range structure of ordinary nuclei would have on other fields of physics, like e.g. nuclear physics of the stars and astrophysics. As a matter of fact, when the distance between the center-of-mass (CM) of two nucleons is about 1 fm, the local density of such a pair is several times larger than that of the central density in nuclei and comparable to that expected in neutron stars; short range correlated NN pairs represent therefore a form of cold dense nuclear matter that can be approached and studied in the laboratory. Such a study, in particular the isospin dependence of SRC, would help to answer several crucial questions on the formation and the structure of neutron stars. As a matter of fact, in spite of the small probability of neutron-neutron (nn) correlations a small concentration of protons inside neutron stars is compensated to a large extent by a significantly larger expected probability of proton-neutron (pn) correlations. In the past decade evidence of SRC has been provided by a new class of experiments based upon the scattering of leptonic and hadronic probes off nuclei at high momentum transfer ($Q^2 > 1\ \mathrm{GeV}^2$). The claimed evidence of SRC in these experiments resulted from: i) the observation of a scaling behaviour of the ratios of inclusive $A(e, e')X$ cross sections on heavy nuclei to those on deuteron,

for values of the Bjorken variable $1.4 \leq x_B \leq 2$ [1], which would indicate that the electron probes two-nucleon correlations in nuclei similar to the ones in the the two body system; ii) the observation of approximate scaling of the ratios of inclusive $A(e,e')\,X$ cross sections on heavy nuclei to those of ^{3}He, for values of the Bjorken variable $2 \leq x_B \leq 3$ [2], which would represent evidence of three-nucleon correlations: iii) the observation of np pairs emitted back-to-back in the process $^{12}C(p,ppn)\,X$ [3] which provided a direct measurement of correlated np pairs, with a yield consistent with the $A(e,e')\,X$ results; moreover, a recent analysis of these data [4] shows that, in agreement with theoretical predictions [5, 6], the high nucleon momentum tail in nuclei is governed by two nucleon SRC dominated by np correlations (in carbon, over 74% of protons with momenta above 275 MeV/c were found to be members of an np correlated pair); iv) the direct observation of pp correlated pairs in a recent JLab experiment [7], where a simultaneous measurement of the triple coincidence ^{12}C $(e,e'pp)\,X$ and the double coincidence ^{12}C $(e,e'p)\,X$ reactions, revealed that the ratio of ^{12}C $(e,e'pp)\,X$ to ^{12}C $(e,e'p)\,X$ events, for proton missing momenta above 300 MeV/c, is $9.5 \pm 2\%$. Further experimental work on SRC is planned, aimed, particularly, at measuring simultaneously the ^{4}He $(e,e'pp)\,X/^4$He $(e,e'p)\,X$, ^{4}He $(e,e'pn)\,X/^4$He $(e,e'p)\,X$, and ^{4}He $(e,e'pn)\,X/^4$He $(e,e'pp)\,X$ ratios for missing momenta in the range 500-875 MeV/c, in order to investigate the hard core region [8]. The experimental results cited above, in particular the large ratio of pn to pp SRC, observed by the EVA/BNL [3] and E01-015 [7] experiments, call for a solid theoretical validation. In Ref. [9] the role of the tensor force in producing a substantial difference between pn and pp two-nucleon momentum distributions in few-body systems and light nuclei ($A < 8$) has been analyzed using *status-of-the-art* realistic nuclear wave functions obtained within the Variational Monte Carlo (VMC) approach [10]. In this paper the results of calculations [11] of the effect of the tensor force on the one- and two-body momentum distributions of medium weight nuclei ($12 \leq A \leq 40$), obtained within a linked cluster expansion and realistic interactions [12, 13], will be presented. In the next section, the cluster expansion method for the one- and two-body densities is outlined; the one- and two-body momentum distributions are illustrated in Section 2; eventually, the results of calculations are presented in Section 3.

1. One- and Two-Body matrices

Within the linked cluster expansion of Ref. [12, 13], the expression for the non diagonal one body density matrix (OBDM) resulting from a correlated ground state wave function of the form $\psi_0 = \phi_0 \prod \hat{f}\,(ij)$ is, in lowest order of $\hat{\eta}_{ij} = \hat{f}_{ij}^2 - 1$:

$$\rho^{(1)}(\boldsymbol{r}_1, \boldsymbol{r}'_1) = \rho^{(1)}_{SM}(\boldsymbol{r}_1, \boldsymbol{r}'_1) + \rho^{(1)}_{H}(\boldsymbol{r}_1, \boldsymbol{r}'_1) + \rho^{(1)}_{S}(\boldsymbol{r}_1, \boldsymbol{r}'_1), \tag{1}$$

where $\rho_{SM}(\boldsymbol{r}, \boldsymbol{r}') = \sum_\alpha \varphi^\star_\alpha(\boldsymbol{r})\,\varphi_\alpha(\boldsymbol{r}')$ is the mean field (MF) density, $\varphi_\alpha(\boldsymbol{r})$ the MF wave function, and $\rho^{(1)}_H$ and $\rho^{(1)}_S$ the hole (H) and spectator (S) correlation contributions, given

respectively by (see Ref. [12])

$$\rho_H^{(1)}(\boldsymbol{r}_1,\boldsymbol{r}'_1) = \int d\boldsymbol{r}_2\,[H_D(\boldsymbol{r}_{12},\boldsymbol{r}_{1'2})\rho_0(\boldsymbol{r}_1,\boldsymbol{r}'_1)\,\rho_0(\boldsymbol{r}_2)+ \\ -H_E(\boldsymbol{r}_{12},\boldsymbol{r}_{1'2})\,\rho_0(\boldsymbol{r}_1,\boldsymbol{r}_2)\,\rho_0(\boldsymbol{r}_2,\boldsymbol{r}'_1)]$$

(2)

$$\rho_S^{(1)}(\boldsymbol{r}_1,\boldsymbol{r}'_1) = -\int d\boldsymbol{r}_2 d\boldsymbol{r}_3\,\rho_0(\boldsymbol{r}_1,\boldsymbol{r}_2)\,[H_D(\boldsymbol{r}_{23})\,\rho_0(\boldsymbol{r}_2,\boldsymbol{r}'_1)\,\rho_0(\boldsymbol{r}_3)+ \\ -H_E(\boldsymbol{r}_{23})\,\rho_0(\boldsymbol{r}_2,\boldsymbol{r}_3)\rho_0(\boldsymbol{r}_3,\boldsymbol{r}'_1)].$$

Here the direct (D) and exchange (E) functions $H_{D,E}$ are the expectation values of the correlation operators with respect to the spin-isospin functions, with the dependence upon the coordinates originating from the spatial part of the correlation functions and from the tensor operator (the explicit expressions are given in Ref. [12]). The non diagonal two-body density matrix (TBDM) can be written as follows:

$$\rho^{(2)}(\boldsymbol{r}_1,\boldsymbol{r}_2;\boldsymbol{r}'_1,\boldsymbol{r}'_2) = \rho^{(2)}_{SM}(\boldsymbol{r}_1,\boldsymbol{r}_2;\boldsymbol{r}'_1,\boldsymbol{r}'_2) + \rho^{(2)}_{2b}(\boldsymbol{r}_1,\boldsymbol{r}_2;\boldsymbol{r}'_1,\boldsymbol{r}'_2)+ \\ + \rho^{(2)}_{3b,1}(\boldsymbol{r}_1,\boldsymbol{r}_2;\boldsymbol{r}'_1,\boldsymbol{r}'_2) + \rho^{(2)}_{3b,2}(\boldsymbol{r}_1,\boldsymbol{r}_2;\boldsymbol{r}'_1,\boldsymbol{r}'_2) + \rho^{(2)}_{4b}(\boldsymbol{r}_1,\boldsymbol{r}_2;\boldsymbol{r}'_1,\boldsymbol{r}'_2),$$

(3)

where $\rho^{(2)}_{SM}$ represents the mean field contribution and the other terms the correlations contributions, with the subscripts $2b$, $3b$ and $4b$ denoting the number of "bodies" (nucleons) involved in the given contribution. The various terms appearing in Eq. (1) are diagrammatically represented in Fig. 1, whereas the diagrams corresponding to the diagonal TBDM (Eq. (3) with $\boldsymbol{r}'_1 = \boldsymbol{r}_1$ and $\boldsymbol{r}'_2 = \boldsymbol{r}_2$) are presented in Fig. 2. The explicit expressions of the diagonal and non-diagonal TBDM are given in Ref. [11] in terms correlation functions and mean field non diagonal one-body density matrices. In case of central correlations and harmonic oscillator (HO) mean field wave functions, analytic expressions of the diagonal TBDM are given in Ref. [14]; when non central correlations are considered, as in the present case, no analytic expression can be given even using HO wave functions.

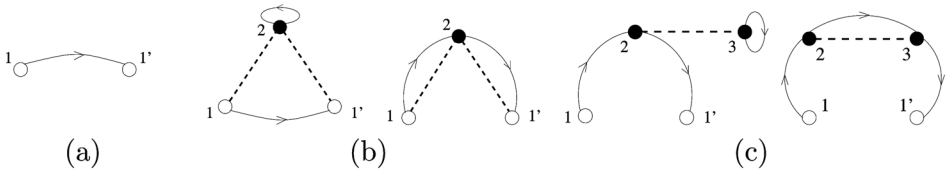

FIGURE 1. – *Diagrammatic representation of the one body mixed density matrix* $\rho^{(1)}(\boldsymbol{r}_1,\boldsymbol{r}'_1)$ *in the lowest order of the η-expansion (Eq. (1)). The three sets of diagrams represent the mean field contribution (a), and the hole (b) and spectator (c) direct and exchange contributions, respectively. Open dots denote the "active" particles; full dots, labeled by an index "i" stand for an integration over the coordinates of particle "i"; an oriented full line, originating from a dot and ending in the same dot, denotes the mean field diagonal OBDM* $\rho_o(i)$*, whereas an oriented full line, joining two different dots, represents the non diagonal OBDM density matrix,* $\rho_o(i,j)$*; dashed lines in* (b) *represent* $\hat{\eta}_{11'2}$ *and those in* (c) $\hat{\eta}_{23}$.

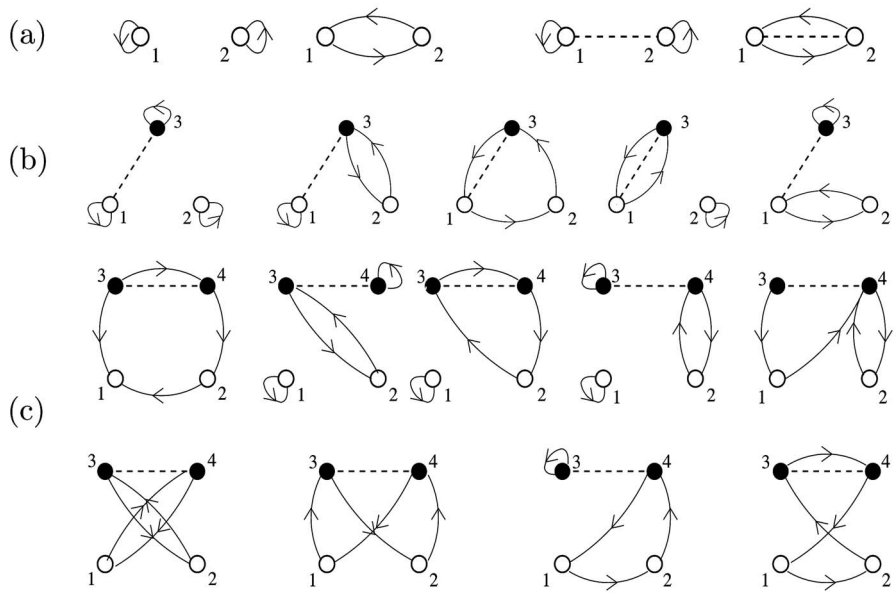

FIGURE 2. – *The same as in Fig.* 1 *for the* diagonal *two-body density matrix (Eq. (3) with* $\boldsymbol{r}'_1 = \boldsymbol{r}_1$ *and* $\boldsymbol{r}'_2 = \boldsymbol{r}_2$*). The groups of diagrams represent the MF + two-* (*a*)*, three-* (*b*) *and four-body* (*c*) *contributions, respectively.*

2. One- and two-nucleon momentum distributions

The one-nucleon momentum distribution (NMD) is the Fourier transform of the OBDM (Eq. (2)), *viz*

$$n(\boldsymbol{k}) = \frac{1}{(2\pi)^3} \int d\boldsymbol{r}_1 \, d\boldsymbol{r}'_1 \, e^{-i\,\boldsymbol{k}\cdot(\boldsymbol{r}_1 - \boldsymbol{r}'_1)} \, \rho^{(1)}(\boldsymbol{r}_1, \boldsymbol{r}'_1), \tag{4}$$

whereas the Fourier transform of the TBDM (Eq. (3)), {*i.e.*}

$$n(\boldsymbol{k}_1, \boldsymbol{k}_2) = \frac{1}{(2\pi)^6} \int d\boldsymbol{r}_1 d\boldsymbol{r}_2 d\boldsymbol{r}'_1 d\boldsymbol{r}'_2 e^{i\boldsymbol{k}_1\cdot(\boldsymbol{r}_1 - \boldsymbol{r}'_1)} e^{i\boldsymbol{k}_2\cdot(\boldsymbol{r}_2 - \boldsymbol{r}'_2)} \rho^{(2)}(\boldsymbol{r}_1, \boldsymbol{r}_2; \boldsymbol{r}'_1, \boldsymbol{r}'_2) \tag{5}$$

represents the two-body momentum distribution (2NMD), which can be written in terms of relative ($\boldsymbol{k}_{rel}$) and Center-of-Mass ($\boldsymbol{K}_{CM}$) momenta as follows

$$\begin{aligned} & n(\boldsymbol{k}_{rel}, \boldsymbol{K}_{CM}) = \\ & = \frac{1}{(2\pi)^6} \int d\boldsymbol{r} \, d\boldsymbol{R} \, d\boldsymbol{r}' d\boldsymbol{R}' \, e^{i\,\boldsymbol{K}_{CM}\cdot(\boldsymbol{R} - \boldsymbol{R}')} \, e^{i\,\boldsymbol{k}_{rel}\cdot(\boldsymbol{r} - \boldsymbol{r}')} \, \rho^{(2)}(\boldsymbol{r}, \boldsymbol{R}; \boldsymbol{r}', \boldsymbol{R}'), \end{aligned} \tag{6}$$

where $\boldsymbol{r} = \boldsymbol{r}_1 - \boldsymbol{r}_2$, $\boldsymbol{r}' = \boldsymbol{r}'_1 - \boldsymbol{r}'_2$, $\boldsymbol{R} = (\boldsymbol{r}_1 + \boldsymbol{r}_2)/2$ and $\boldsymbol{R}' = (\boldsymbol{r}'_1 + \boldsymbol{r}'_2)/2$. The relative, $n_{rel}(\boldsymbol{k}_{rel})$, and CM, $n_{CM}(\boldsymbol{K}_{CM})$, momentum distributions can be obtained from Eq. (6) integrating over $\boldsymbol{K}_{CM}$ and $\boldsymbol{k}_{rel}$, respectively.

3. Results and Conclusions

In the numerical calculations we have considered the case of $A = 12, 16$ and 40. The ingredients we need for the calculations are the single particle MF wave functions and the correlation functions, appearing in Eqs. (1) and (3). The correlation functions we have used include central, spin, isospin and tensor correlations and correspond to the $V8'$ realistic interaction [15]; the MF wave functions, whose parameters were fixed by minimizing the ground state energy (see [12]), have been chosen both in the Woods-Saxon form. The momentum distributions of ^{12}C, ^{16}O and ^{40}Ca are shown in Fig. 3, where they are compared with the results of higher order calculations, e.g. the Variational Monte Carlo and Fermi Hyper Netted Chain ones. The results for the diagonal TBDM are shown in Fig. 4, and the *pn*, *pp* and total two-body momentum

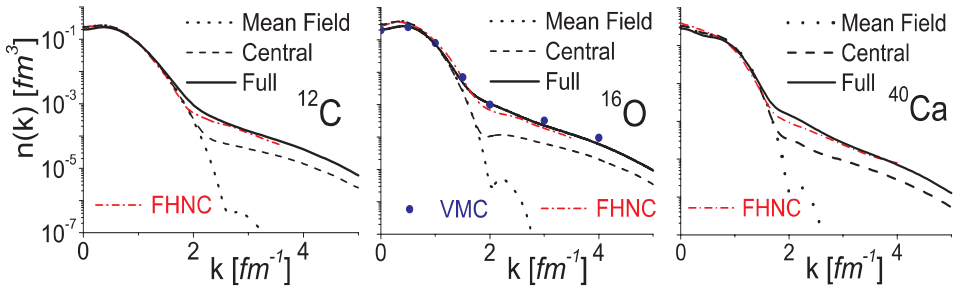

FIGURE 3. – *The one-nucleon momentum distribution calculated within the cluster expansion of Ref. [12] (dots, dashes and full)) compared with the VMC results of Ref. [16] (full dots) and the FHNC results of Ref. [17] (dot-dashes).*

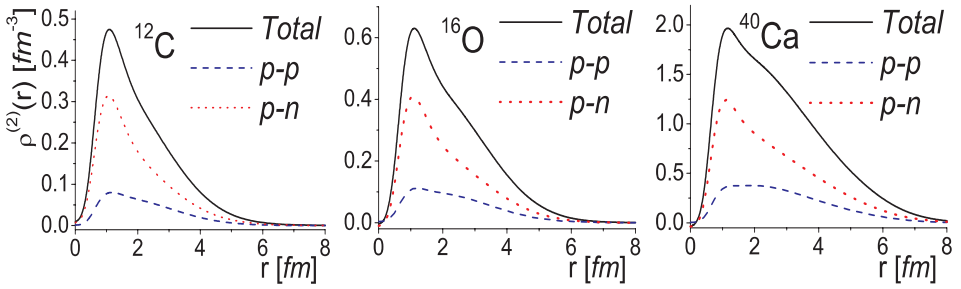

FIGURE 4. – *The relative two-body density distribution (Eq. (3) with* $\boldsymbol{r}'_1 = \boldsymbol{r}_1$ *and* $\boldsymbol{r}'_2 = \boldsymbol{r}_2$*) integrated over the CM coordinate* $\boldsymbol{R} = (\boldsymbol{r}_1 + \boldsymbol{r}_2)/2$*). The proton-neutron (pn) and proton-proton (pp) contributions are also shown. The various curves are normalized to the corresponding numbers of NN pairs of the given type.*

distributions are shown in Figs. 5 and Fig. 6; eventually, in Fig. 7 the extent to which the 2NMD factorizes into the relative and CM momentum distributions is illustrated. The factorization of the 2NMD has been used in Ref. [6] to obtain the one nucleon spectral function of complex nuclei at high values of momenta and removal energies.

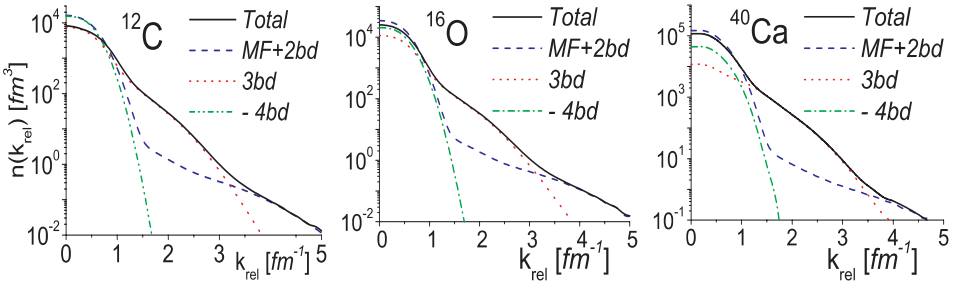

FIGURE 5. – *The relative two-body momentum distribution (Eq. (6)) integrated over* $\boldsymbol{K}_{CM}$. *The various contributions corresponding to the diagrams in Fig.* 2 *are also shown.*

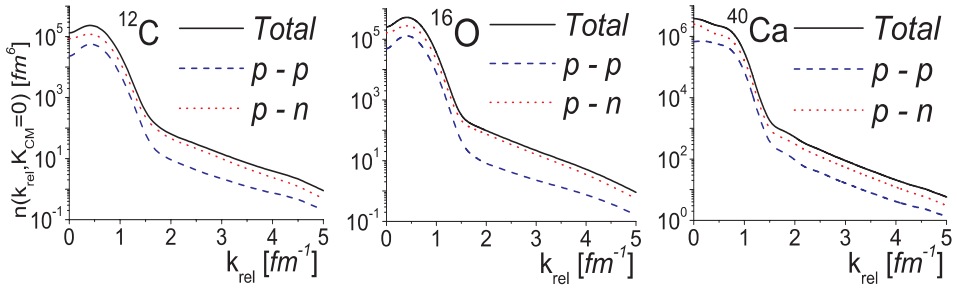

FIGURE 6. – *The relative two-body momentum distribution (Eq. (6)) calculated in correspondence of* $\boldsymbol{K}_{CM} = 0$ *(back-to-back nucleons).*

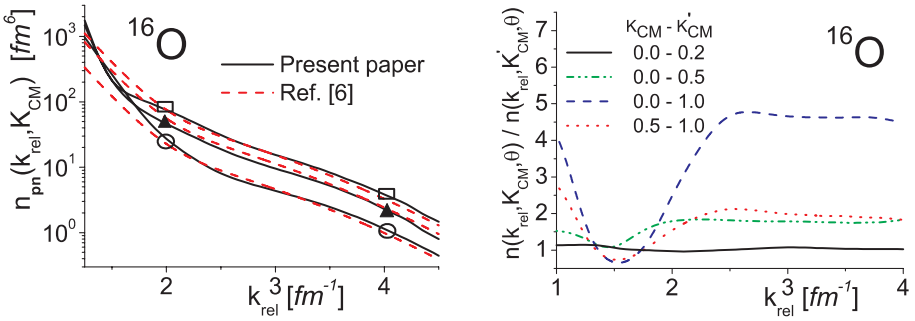

FIGURE 7. – *Check of the factorization assumption of the* 2*NMD. Left: the exact* 2*NMD of the present paper compared with the factorized form of Ref. [6]* $n\,(\boldsymbol{k}_{rel}, \boldsymbol{K}_{CM}) = C_A\; n_D(k_{rel})$, $n_{CS}(K_{CM})$ *(see text); the values of* K_{CM} *corresponding to the various curves are* $K_{CM} = 0\,fm^{-1}$ *(squares),* $0.5\,fm^{-1}$ *(full triangles),* $1\,fm^{-1}$ *(open dots). Right: the ratio* $n(k_{rel}, K_{CM}, \theta)/n\,(k_{rel}, K'_{CM}, \theta)$ *for various values of* K_{CM} *and* K'_{CM} *and a fixed value of* $\theta = 90^o$ *(see text).*

We have checked such a factorization assumption by: i) comparing the exact 2NMD with the factorized form used in [6], *viz* $n(\boldsymbol{k}_{rel}, \boldsymbol{K}_{CM}) = C_A\; n_D(k_{rel})\, n_{CS}(K_{CM})$, where $n_D(k_{rel})$ is the deuteron momentum distribution and $n_{CS}(K_{CM})$ the CM distribution given in [6]; ii) by analyzing the ratio $n(k_{rel}, K_{CM}, \theta)/n(k_{rel}, K'_{CM}, \theta)$ for various values of K_{CM}, K'_{CM}, and fixed value of $\theta \equiv \theta_{\widehat{kK}} = 90^o$.

The main results we have obtained can be summarized as follows:

- the high momentum part of the nucleon momentum distributions clearly exhibits the effects of tensor correlations, which can be very reliably described within the lowest order cluster expansion we have developed (cf. Fig. 3) (the effects of the higher order terms is negligibly small (see Ref.[12]);
- in agreement with the results for light nuclei [9], at relative momentum $k_{rel} \geq 1.5\, fm^{-1}$ the momentum distribution of pn pairs is much larger than that of pp pairs (cf. Fig. 5), whereas at small values of k_{rel} the ratios of pn and pp momentum distributions is similar to the ratio of the number of pn to pp pairs, which is 12/5, 16/7 and 40/19 for ^{12}C>, ^{16}O and ^{40}Ca, respectively;
- our parameter-free many-body approach confirms the validity of the factorization approximation of the 2NMD at high values of the relative momentum and low values of the CM momentum (*cf.* Fig. 7).

References

[1] L.L. Frankfurt, M.I. Strikman, D.B. Day and M. Sargsian, Phys. Rev., **C48** (1993), 2451.
[2] K.S. Egiyan *et al.* (CLAS), Phys. Rev. Lett., **96** (2006), 082501.
[3] A. Tang *et al.*, Phys. Rev. Lett., **90** (2003), 042301.
[4] E. Piazetsky, M. Sargsian, L. Frankfurt M. Strikman and J.W. Watson, Phys. Rev. Lett., **97** (2006), 162504.
[5] L. Frankfurt and M. Strikman, Phys. Rep., **76** (1981), 214.
[6] C. Ciofi degli Atti and S. Simula, Phys. Rev., **C53** (1996), 1689.
[7] R. Shneor *et al.*, Phys. Rev. Lett., **99** (2007), 072501.
[8] E. Piazetsky and D. Higinbotham, JLab experiment E07-006 (2007).
[9] R. Schiavilla, R.B. Wiringa, S.C. Pieper and J. Carlson, Phys. Rev. Lett., **98** (2007), 132501.
[10] R.B. Wiringa and S.C. Pieper, Phys. Rev. Lett., **89** (2002), 182501.
[11] M. Alvioli, C. Ciofi degli Atti and H. Morita, to appear.
[12] M. Alvioli, C. Ciofi degli Atti and H. Morita, Phys. Rev., **C72** (2005), 054310; Fizica, **B13** (2004), 585.
[13] M. Alvioli, C. Ciofi degli Atti and H. Morita, in *Science and Supercomputing in Europe 2005*; Alberigo, Erbacci and Garofalo Editors, Bologna (2005).
[14] S.S. Dimitrova, D.N. Kadrev, A.N. Antonov and M.V. Stoitsov, Eur. Phys. J., **A7** (2000), 335.
[15] R.B. Wiringa, V.G.J. Stocks and R. Schiavilla, Phys. Rev., **C51** (1995), 38.
[16] S.C. Pieper, R.B. Wiringa and V.R. Pandharipande, Phys. Rev., **C46**, 1741 (2000).
[17] C. Bisconti, F. Arias De Saavedra and G. Có, nucl-th/0702061.